Serial Course of Left Ventricular Function, Perfusion and Fatty Acid Uptake in the Cardiomyopathic Hamster

Kenji Nakai,* Marsood Ahmad, Motoe Nakaki, Robert Wilkinson, Ronald J. Callahan, David R. Elmaleh, Alan J. Fischman and H. William Strauss

Division of Nuclear Medicine, Massachusetts General Hospital, and Department of Radiology, Harvard Medical School, Boston, Massachusetts

To determine the relationship of metabolic and perfusion changes to alterations in ventricular function in the course of cardiomyopathy, we performed serial measurements of ejection fraction, myocardial perfusion, fatty acid uptake of 3-methyl-p[^{123}I]-phenyl-pentadecanoic acid ([^{123}I]3MPDA) and myocardial histology in Syrian hamsters genetically predisposed to the development of congestive cardiomyopathy (Bio T0-2) (n = 30) and normal age-matched control animals (Bio F1B) (n = 13). To obtain high-resolution information about the myocardium at the time of onset of the first noticeable decrease in ventricular function, a multitracer autoradiographic study using ^{99m}Tc-pyrophosphate, ^{201}Tl and [^{14}C]3MPDA was obtained at 90 days of age. Baseline ejection fraction recorded at 60 days averaged 60.3%; by 90 days, it decreased to 54.3% ($p < 0.05$), falling to 41.3% at 180 days ($p < 0.01$) and declining to 30% at the end of the study. A progressive increase in the extent of myocytolysis, fibrosis and calcification was seen in the histologic studies as the animals aged. The ratio of fatty acid-to-thallium uptake dropped from 0.51 ± 0.09 to 0.45 ± 0.11 ($p < 0.01$), which is in parallel with the reduction in ejection fraction. The thallium lung-to-heart ratio increased from 0.51 at 90 days to 0.59 at 270 days ($p < 0.05$), which corresponds to the worsening of cardiac function. The macroautoradiographic studies demonstrated slight uptake of pyrophosphate in the myopathic hamster hearts and minimal changes in the regional distribution of fatty acid compared to that of perfusion. We conclude that the decrease in ventricular function parallels the severity of myocytolysis and fibrosis. Although decreased fatty acid uptake was apparent at an early stage, the extent of the change is modest and is difficult to detect from external images.

J Nucl Med 1993; 34:1309–1315

Primary congestive cardiomyopathy is a disease of the heart muscle of unknown etiology. Depending on the stage and severity of the illness, global and regional function may be normal or depressed. While perfusion is generally normal in the early phases, several investigators have reported focal perfusion abnormalities in the absence of coronary artery disease (*1*). In advanced cardiomyopathy, marked changes of fatty acid and glucose metabolism have been observed (*2*). Whether the metabolic changes precede the reduction of ventricular function or are a consequence of reduced function is uncertain. To understand this relationship, serial measurements beginning prior to the clinical manifestation of the illness are required.

A strain of Syrian hamster develops congestive cardiomyopathy due to a genetic abnormality, with phenotypic expression in 100% of the affected line (*3–5*). On histologic examination, the myocardium appears normal, at least through 30 days of age in the female and 45 days in males; spotty cellular myocytolysis with little surrounding inflammatory reaction occurs over the next 30–60 days (*3*). By 60 days of age, the maximum force of contraction (dF/dt) is slightly depressed from that measured earlier (*3*) and probably represents the first manifestation of the depressed ventricular function. In a preliminary study, we found no discernible reduction in ventricular function through 60 days of age (*6*). The cause of myopathy is not well understood, but appears to involve an alteration in the cellular handling of calcium. Previous studies have shown a reduction in myocyte necrosis when the animals are treated with the calcium channel blocker, verapamil (*7,8*).

To determine the relationship of metabolic and perfusion changes to altered ventricular function, we studied four groups of hamsters at different ages. One group, examined at 90 days of age, was evaluated with macroautoradiography to determine the relative distribution of perfusion and fatty acid uptake in the endocardium and epicardium. In addition, to determine if the changes in calcium uptake could be detected, measurements were also studied with ^{99m}Tc-pyrophosphate. The remaining three groups of animals had radionuclide imaging studies of the myocardial distribution of modified fatty acid and ^{201}Tl recorded in parallel with determinations of ejection fraction. The animals were studied at 90–120 days, 180–210 days and 270–300 days of age. To define the relationship of metabolic and

Received Jun. 29, 1992; revision accepted Mar. 4, 1993.
For correspondence or reprints contact: H. William Strauss, MD, Bristol-Myers Squibb Co., P.O. Box 4000, Princeton, NJ 08543-4000.
*Present address: Clinical Pathology & Second Internal Medicine, Iwate Medical University, Morioka, Japan 020.

function measurements to myocardial histology, the hamsters were killed after radionuclide measurement at each stage, their hearts were removed, fixed in formalin and stained for evaluation by light microscopy.

Fatty acid uptake was measured with a branched-chain fatty acid designed to prolong the retention of the agent in the heart. A methyl group substituted for hydrogen on carbon three prevents the initial cycle of beta-oxidation by precluding formation of the keto-acyl Co-A (*9–12*). The branched chain fatty acid enters the myocardial metabolic pathway in proportion to palmitate, but is retained in the tissue, probably in the form of triglycerides. A comparison of ^{11}C labeled 3-methyl heptadecanoic acid (3MHDA) to ^{14}C-palmitate demonstrated similar initial uptake of the two agents, suggesting that 3MHDA paralleled the uptake of long-chain fatty acid (*10*). Analogues of 3MHDA were synthesized with the phenyl group in the omega position to permit iodination for single-photon imaging. In this study, we used 3-methyl-p[^{123}I]-phenyl-pentadecanoic acid ([^{123}I]3MPDA), a modified fatty acid with the highest myocardial uptake, longest myocardial retention and kinetics similar to those of 3-methyl heptadecanoic acid.

MATERIALS AND METHODS

Animal Model

Male Syrian hamsters destined to develop cardiomyopathy strain Bio T0-2 (formerly called Bio 53.58) (n = 33) and age-matched normal control hamsters (Bio F1B) (n = 13) were evaluated. All animals had baseline ventricular function measurements at 60 days of age and follow-up measurements at later times as indicated below.

Macroautoradiography

Autoradiographic studies were performed in nine hamsters at 90 days of age (five myopathic, four controls) to determine the distribution of fatty acid uptake, perfusion and to identify zones of necrosis, presumably from calcium overload. Carbon-14-labeled 3-methyl-p-phenyl-pentadecanoic acid ([^{14}C]3MPDA) was synthesized as previously described (*12*). The animals received three radiopharmaceuticals via intravenous (penile) injection: 30 mCi of ^{99m}Tc-pyrophosphate (PYP) followed ~3 hr later by coinjection of 500 μCi of ^{201}Tl and 25 μCi of [^{14}C]3MPDA. The animals were killed 30 min later*, their hearts removed, frozen in liquid nitrogen and sectioned with a cryomicrotome. Tissue sections of 16 micron thickness were placed on Kodak x-ray single emulsion film for exposure and developed using a standard x-ray processor. The first exposure started within 6 hr of death and lasted for 3 hr to define the distribution of ^{99m}Tc-PYP. The second exposure, initiated 2 days later, following the decay of ^{99m}Tc-PYP activity, revealed ^{201}Tl distribution. The third exposure, initiated 4 wk later, required 10 days to record the distribution of [^{14}C]3MPDA. The regional distribution of [^{14}C]3MPDA was compared with that of ^{201}Tl and ^{99m}Tc-PYP.

*Thirty minutes was selected for death because preliminary studies demonstrated a surprisingly long circulation time for the modified fatty acid. In contrast to the usual half-time of blood clearance of <2 min in other species, the hamsters had a half-time of >10 min.

Electrocardiography

Electrocardiograms were recorded at the time of blood-pool imaging using the standard limb and augmented unipolar lead system; precordial leads were placed approximately at the manubrium and on the left mid-chest. EKGs were evaluated for the electrical axis, presence of P waves, size and configuration of the QRS complex and the presence of ST-segment abnormalities and T-waves.

Scintillation Camera Studies

Modified Fatty Acid. Labeling of 3MPDA with ^{123}I was accomplished by isotope exchange using acetic acid as the solvent and $CuSO_4$ as the catalyst. The radiochemical yield exceeded 96% (determined by thin-layer chromatography). The labeled product was dried and dissolved in a human serum albumin/saline solution. The solution was sterilized by filtration (Millipore 0.22 μm).

Phantom Study

To determine whether data recorded with a dual-tracer collection requires correction for crossover of activity from one tracer window to the other, sources of ^{201}Tl and ^{123}I (25 μCi) were placed in petri dishes and imaged at both the iodine and thallium windows.

Imaging Studies

All radionuclide images were recorded with a large field of view scintillation camera (Technicare 410, Technicare Co., Solon, OH) equipped with a pinhole collimator and 3-mm aperture. Data from the scintillation camera were recorded in a dedicated computer system (MCS 560, Technicare Co., Solon, OH).

Blood-Pool Images

Left ventricular ejection fraction (LVEF) was assessed by multigated blood-pool images recorded at 60, 90–120, 180–210 and 270–300 days of age. All animals were examined at their time of arrival in the laboratory (60 days of age) and the time of death. Following intravenous (penile) injection of 20 mCi of ^{99m}Tc-IgG (*6*) the pinhole was positioned to optimize magnification (about 1 cm from the chest), with the heart centered in the field of view. Electrodes were attached to the limbs and the EKG was evaluated for adequate gating. The typical heart rate was <100 bpm. The cardiac cycle was divided into 24 frames (64 × 64 matrix); data were recorded in the anterior projection for 600 sec/acquisition. LVEF was calculated manually as previously described (*6*). Briefly, after background subtraction, regions of interest (ROIs) were drawn over the left ventricular blood-pool at end-systole and end-diastole, and the resultant counts in each region were used to calculate ejection fraction.

Thallium-201 and [^{123}I]3MPDA Images

The animals were fasted for at least 12 hr prior to injection. Perfusion and fatty acid images were recorded following co-injection of 500 μCi of ^{201}Tl and 500 μCi of [^{123}I]3MPDA. The pinhole was positioned to optimize magnification (about 1 cm from the chest) with minimal distortion. The left ventricle was centered in the field of view. Thallium-201 images were recorded within 5 min of injection at the 80 keV mercury x-ray with a 20% window followed by the iodide data within 30 min of injection with a 20% window centered at 159 keV. The perfusion and modified fatty acid images were recorded in a 128 × 128 matrix for a preset time of 10 min each.

For each ^{201}Tl and [^{123}I]3MPDA image pair, the total heart uptake of radiopharmaceutical was determined from the total myocardial ROI after interpolated background subtraction and

normalization for the injected dose. The lung-to-heart uptake ratio was measured for ^{201}Tl from ROIs set over the anterior wall of the myocardium and the upper portion of the left lung field.

Histologic Findings

At the conclusion of the imaging studies, the hamsters were anesthetized with phenobarbital, killed, and the hearts were removed, fixed in 3.7% buffered formaldehyde, embedded and cut into 5-μm thick sections. The specimens were stained with hematoxylin-eosin and Masson's trichrome stains and examined for fibrosis and myocytolysis.

Statistical Analysis

Results are expressed as mean ± s.d. and are analyzed with unpaired t-test when appropriate. Statistical significance was taken as $p < 0.05$.

RESULTS

Macroautoradiography

Multitracer autoradiography demonstrated a uniform distribution of perfusion, but a minimal decrease in the subendocardial uptake of fatty acid in the four myopathic hamsters at 90 days (Fig. 1). Several small focal zones of mid-myocardial pyrophosphate uptake were observed in the left ventricle of each myopathic hamster. No pyrophosphate accumulation was observed in four control hamsters.

Phantoms

The crossover contribution of ^{201}Tl (80 keV) to the ^{123}I window (159 keV) was 14% with 25 μCi in the field of view. Under these circumstances 1% of iodine counts were found in the thallium window. Assuming 2%–4% of the administered dose of each tracer localized in the myocardium, less than 15% of the measured counts of thallium would appear in the iodine window. Based on these observations, no correction for crossover was performed.

Electrocardiography

The electrocardiographic study showed decreased QRS amplitude, left-axis deviation of the spatial vector and flat T-waves. These changes were observed on the initial tracings recorded at 120 days and progressed as the hamsters aged. Representative ECGs are shown in Figure 2.

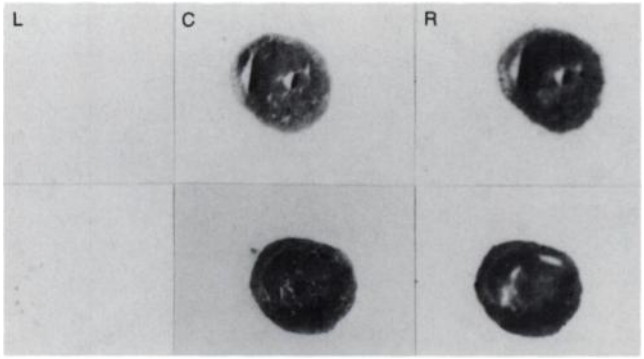

FIGURE 1. Multitracer autoradiography of mid-ventricular specimens of age-matched controls (top) and myopathic hamsters (bottom). Technetium-99m-PYP is depicted in the left hand panels, ^{201}Tl in the center and [^{14}C]3MPDA on the right. No accumulation of ^{99m}Tc-PYP is seen and there is uniform distribution of ^{201}Tl and [^{14}C]3MPDA in the 90-day-old normal control. Note the mild ^{99m}Tc-PYP uptake in the periphery of the myocardium and the minimal mismatch between ^{201}Tl and [^{14}C]3MPDA in the subendocardial region of the age-matched Syrian hamster.

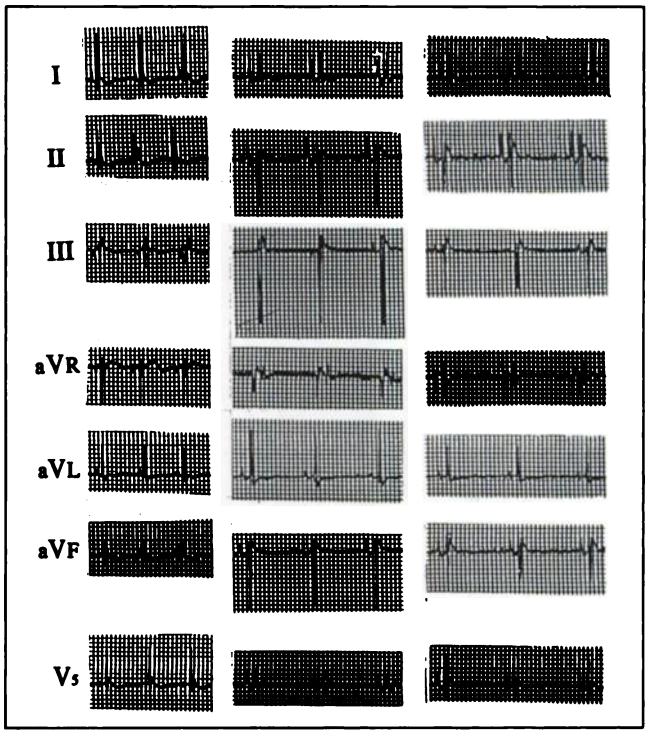

FIGURE 2. Representative electrocardiograms of lead I, II, III, aVR, aVL, aVF and V5 as indicated. The left column are data recorded in a normal control hamster at 210 days of age; middle: cardiomyopathic hamster at 210 days of age; and right: Cardiomyopathic hamster at 270 days of age. Note decreased QRS amplitude, left axis deviation of the spatial vector and flat T-waves. These changes began on the initial tracings recorded at 180 days and progressed with increasing of age.

In Vivo Imaging Studies

Thirty-three myopathic hamsters and 13 normal hamsters were evaluated. The myopathic group (n = 11), evaluated at 90 to 120 days, continued to gain weight and appeared healthy. The myopathic animals (n = 11), evaluated at 180–210 days, did not appear as robust as those in the earlier study, but continued to gain weight. The animals evaluated at 270–300 days appeared ill, failed to continue gaining weight and had gross evidence of ascites (n = 11).

Gated Blood-Pool Scans

LVEF in the myopathic hamsters decreased from 60.3% ± 7.2% initially, to 54.3% ± 7.2% ($p < 0.05$) by 90 days, 41.3% ± 5.7% ($p < 0.01$) by 180 days and declined further to 30% ± 6.3% ($p < 0.01$) at the end of the study. LVEF in the age-matched normal hamsters did not change significantly (64.8% ± 6.2%, 63.4% ± 3.1%, 62.3% ± 3.6% and 63.3% ± 3.3%) (p = ns), respectively (Table 1). The decline in ejection fraction was accompanied by dilatation of the left ventricle and a decrease in wall motion.

Thallium and Fatty Acid Images

Although the autoradiographs demonstrated minor differences between thallium and fatty acid prior to 90 days of

TABLE 1
Serial Changes in LVEF

	Early stage (60 days)	Early stage (90–120 days)	Middle stage (180–210 days)	Late stage (270–300 days)
Control	64.8 ± 6.2	63.4 ± 3.1	62.3 ± 3.6	63.3 ± 3.3
	NS	$p < 0.05$	$p < 0.01$	$p < 0.01$
Myopathic	60.3 ± 7.2	54.3 ± 7.2	41.3 ± 5.7	30.3 ± 6.3
	NS	$p < 0.01$	$p < 0.01$	

age, the in vivo images did not demonstrate significant heterogeneity until 180–210 days of age. Quantitative analysis of the ^{201}Tl-to-fatty acid uptake ratio is shown in Table 2. The count ratios between fatty acid and ^{201}Tl changed in the myopathic: 0.51 ± 0.09 at 90–120 days old ($p < 0.05$), 0.49 ± 0.10 at 180–210 days ($p < 0.01$), 0.45 ± 0.11 at 270–300 days old ($p < 0.01$), but remained constant in the control animals: 0.60 ± 0.01 at 90–120 days old, 0.61 ± 0.06 at 180–210 days old, 0.58 ± 0.05 at 270–300 days old (Table 2). Representative examples are shown in Figure 3.

Thallium-201 lung-to-myocardial ratios in normal hamsters averaged 0.43. Thallium-201 lung-to-myocardial ratio in the myopathic hamsters was elevated at 0.51 ± 0.06 early in the study when the animals were 90–120 days of age ($p < 0.01$). The ratio increased slightly to 0.52 ± 0.07 at 180–210 days old and rose significantly to 0.59 ± 0.05 ($p < 0.05$) at 270 days in the myopathic hamsters (Table 3). No significant changes were noted in the normal control animals (0.43 ± 0.09 at 90–120 days old, 0.43 ± 0.03 at 180–210 days old, 0.44 ± 0.04 at 270–300 days old).

Histologic Findings

Light microscopic observations of the heart in cardiomyopathic Bio T0-2 Syrian hamsters revealed progressive changes. The changes consisted of focal myocytolysis with concurrent healing by fibrous tissue replacement and myocellular and interstitial calcification. Foci of myofibrillar degeneration (myocytolysis and partial calcification) were observed initially at 90 days. In the 180-day-old myopathic hamsters, there was an increase in myocytolysis with fibroblasts. At 300 days of age, active myocytolysis had diminished, and there was more pronounced healing and ventricular scarring, and hypertrophy. Representative cases are shown in Figure 4.

DISCUSSION

Previous work by Bajusz et al. demonstrated that cardiac muscle lesions developed in 100% of Bio 14.6 Syrian hamsters (*13*). Although the first dystrophic inborn lines were noted accidentally from animals of the Bio 1.50 line, several cardiomyopathic lines are now maintained from the BIO 14.6 line (*14*). These animals have a mean life expectancy of 12 mo. During the first phase of disease, no clinical or gross pathologic changes occur. As the animals age, they develop EKG changes that are manifested by alterations in the QRS complex and spatial vector in parallel with the development of the histologic lesions (*4*). In the present experiment, changes of left-axis deviation, enlargement of P-waves and low voltage in the QRS complex suggested ventricular overload and loss of myocardial cells. These changes correspond to a marked reduction of ventricular function, decreasing from a baseline value of 60.3% to 41% by 180 days of age.

Histologic lesions have not been seen by light microscopy in Syrian hamster myopathic hearts before the 45th day of life, although ultrastructural studies of cardiomyopathic heart revealed focal dissolution of myofilaments in male animals at 30 days of age and female animals at 50 days of age (*15*). By 60 days, focal myocytolysis with little surrounding inflammatory reaction begins in both sexes. Foci of myofibrillar degeneration were observed most frequently between 50 and 150 days of age and continued to increase to 180 days of age. These histologic changes were observed prior to the onset of clinical signs of congestive heart failure. In our experiment, foci of myofibrillar degeneration (myocytolysis and partial calcification) were observed at 60–90 days. The abnormal uptake of pyrophosphate seen on autoradiography at 90 days is probably a reflection of histological calcification. LVEF was slightly

TABLE 2
Serial Changes in Total Count Ratio Between Fatty Acid and ^{201}Tl

	Early stage (90–120 days)	Middle stage (180–210 days)	Late stage (270–300 days)
Control	0.60 ± 0.1	0.61 ± 0.06	0.58 ± 0.05
	$p < 0.05$	$p < 0.01$	$p < 0.01$
Myopathy	0.51 ± 0.09	0.49 ± 0.10	0.45 ± 0.11
	NS	$p < 0.05$	
	$p < 0.01$		

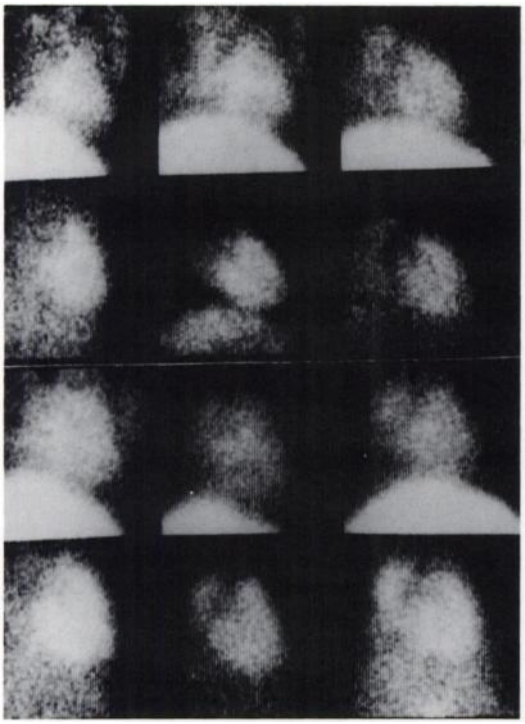

FIGURE 3. Representative [^{123}I]3MHDA (rows 1 and 3) and ^{201}Tl images (rows 2 and 4) in the anterior projection in a normal hamster (top two panels) and a myopathic hamster (bottom two panels). Data in the left hand column were recorded at 90–120 days of age; in the center column at 180–210 days; and at 270–300 days on the right. Note the modest changes in myocardial fatty acid uptake over time. At the beginning of the study, the myopathic animals had high lung uptake of fatty acid. The ratio of heart-to-liver (in the images) and absolute myocardial fatty acid uptake (summarized in Table 2) indicates the decline in myocardial fatty acid uptake. Thallium uptake, on the other hand, remains relatively unchanged throughout the study.

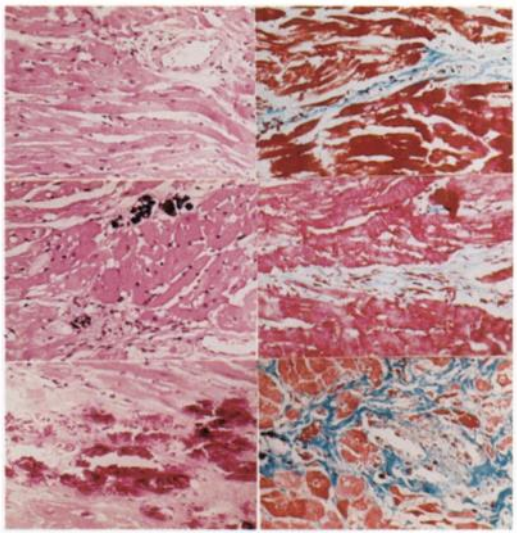

FIGURE 4. Samples of histologic sections from representative myopathic animals studied at 90–120 days (upper), 180–210 days (middle) and 270–300 days (bottom). The specimens on the left were stained with H&E, whereas those on the right were stained with Masson's trichrome. Early in myopathic course, minimal changes are evident. The specimen in the upper panel demonstrated slight myocytolysis with minimal calcification and fibrosis. At 180–210 days (center panel), focal degeneration (myocytolysis and calcification) is more apparent and fibrosis is more extensive. The specimen on the bottom demonstrates marked fibrosis and numerous dark staining calcium granules both intracellularly and extracellularly.

reduced at this time. Although it is difficult to relate these histologic changes directly to altered fatty acid uptake and myocardial perfusion, we observed a decrease of global fatty acid uptake and foci of abnormal pyrophosphate uptake in myopathic hamsters at 90 days. This parallels initial observations of decreased function.

Although the precise genetic defect in the Syrian hamster has not been determined, calcium overload of myocytes has been implicated in the etiology of cardiac abnormalities in these hamsters (*16*). Several studies have shown that the abnormalities in voltage-dependent calcium channels play a role in the pathophysiology of cardiomyopathic hamsters (*17–19*). Kuo et al. reported that the imbalance in Ca^{2+} flux followed by a selective decrease of Ca^{2+}-pumping ATPase activity may be involved in the pathogenesis of this cardiomyopathy (*20*). The presence of electron-dense calcium apatite granules within mitochondria and our observation of pyrophosphate uptake supports the concept that an overload of cellular calcium plays a role in the process. Accumulation of ^{99m}Tc-pyrophosphate suggests irreversible injured myocardium probably due to calcium overload of myocytes (*21*). On the other hand, Factor et al. suggested that microvascular spasm may be a common denominator of many different cardiomyopathic syndromes (*22*). The relatively normal regional and global distribution of ^{201}Tl in myopathic animals, however, makes this unlikely. The fact that treatment with verapamil has been effective in preventing abnormalities of cardiac function and histopathology (*23,24*) in these animals provides additional evidence that abnormal handling of this ion plays a significant role in the evolution of this disorder.

Long-chain fatty acids are the principle substrate of myocardial metabolism. Under aerobic conditions, most fatty acids are rapidly catabolized by beta-oxidation (*25*).

TABLE 3
Serial Changes in ^{201}Tl Lung-to-Myocardial Ratio

	Early stage (90–120 days)	Middle stage (180–210 days)	Late stage (270–300 days)
Control	0.43 ± 0.04	0.43 ± 0.03	0.44 ± 0.04
	$p < 0.01$	$p < 0.05$	$p < 0.01$
Myopathy	0.51 ± 0.06	0.52 ± 0.07	0.59 ± 0.05
	NS	$p < 0.05$	

Significant changes in fatty acid metabolism occur under conditions of hypoxia and ischemia (*26*). The branched-chain modified fatty acid analog used in this study, 3MHDA, is metabolically "trapped" in the myocardium following the formation of acyl CoA (*8*). Theoretically, beta-oxidation beyond the third enzymatic step in the four enzyme beta-oxidation pathway cannot occur due to the 3-methyl group substitution (*27*). The importance of fatty acid utilization was demonstrated by Aswitto et al. These investigators found that within a few hours of birth, pig hearts are able to oxidize long-chain fatty acids and that the rate of oxidation is linked to mechanical function (*28*). Furthermore, a decrease in fatty acid oxidation after coronary occlusion causes a marked decrease in myocardial tension development (*29*) and the accumulation of fatty acyl-CoA and acyl carnitine esters in the cytosol (*30*). Thus, fatty acid metabolism can serve as an indicator of myocardial energetic efficiency (*8*). Goldstein et al. demonstrated that the clearance rate of ^{11}C-palmitate from rabbit myocardium can serve as index for whole heart metabolism of fatty acids (*30*). In studies with ^{11}C-palmitic acid and other long straight-chain ^{11}C-labeled fatty acids, there is fast washout of activity from the myocardium due to beta-oxidation, which requires rapid, serial imaging to determine the metabolic rate. Alpha and omega oxidation seem to make only a small contribution to fatty-acid metabolism in the myocardium (*31*). Livni et al. demonstrated that ^{14}C-heptadecanoic acid (HDA) is trapped in proportion to palmitic acid in the myocardium and might therefore be used for studies of myocardial fatty acid uptake (*9*).

In this study, we used [^{123}I]3MPDA, a modified fatty acid with the highest myocardial uptake, longest myocardial retention and kinetics similar to those of 3-methyl heptadecanoic acid. Perfusion and modified fatty acid uptake are closely coupled and have a similar pattern of distribution in normal myocardium (*32,33*). Furthermore, Miller et al. reported that accumulation of the branched-chain fatty acid analog was characteristic of ischemically "stunned" but viable myocardium (*34*). When both fatty acid and perfusion were decreased, the myocardium was damaged irreversibly. In the myopathic animals reported here, a different pattern was observed, fatty acid uptake was globally reduced and heterogeneous, especially at the late phases of illness when the animals had ascites and appeared grossly ill (*35*). Whether the reduction in fatty acid uptake was due to substitution of another substrate, such as glucose, cannot be stated from the present experiment. The decrease in ventricular function associated with a decrease in fatty acid uptake, however, suggests that myocardial metabolism may be globally reduced.

CONCLUSION

This study demonstrated progressive changes in left ventricular function which paralleled alterations in the histology of the left ventricle in cardiomyopathic Syrian hamsters. On the initial images, myocardial perfusion and fatty acid uptake were nonhomogeneous and autoradiographic studies of 90-day-old hamsters demonstrated slight subendocardial loss of fatty acid uptake. At this time, focal zones of pyrophosphate localization were seen in the mid-myocardium of the myopathic animals. Although these changes were apparent on the autoradiographs, they were not visible on in vivo pinhole images (data not shown). By 90 days of age, the LVEF had decreased significantly, although slightly from control values. By 180 days of age, LVEF had decreased substantially and continued to fall to the end of the study.

Our studies suggest that myocardial metabolism was altered at a very early stage in the natural history of this disease, which parallels alterations in histology and function. Myocardial perfusion remains essentially unchanged as the animals develop heart failure. Although this study suggests that metabolic changes occur in parallel with a reduction of ventricular function, the changes are modest and are difficult to detect by imaging. Determination of the relationship of regional perfusion to fatty acid uptake may be useful as an additional parameter of altered function in this animal model of cardiomyopathy, but it is not likely to be more sensitive than determination of ventricular function.

REFERENCES

1. Bulkey BH, Hutchins GM, Bailey I, Strauss HW, Pitt B. Thallium-201 imaging and gated cardiac pool scan in patients with idiopathic cardiomyopathy. A clinical and pathologic findings. *Circulation* 1977;55:753.
2. Schelbert HR, Selin C, Marshall RC. Regional myocardial ischemia assessed by ^{18}F-fluoro-2-deoxyglucose and positron emission computed tomography. In: Kreuzer H, Parmley WW, Rentrop P, Heiss HW, eds. *Advances in clinical cardiology, volume I. Qualification of myocardial ischemia*. New York: Witzrock; 1980:437–449.
3. Strobeck JE, Factor SM, Bhan A, et al. Hereditary and acquired cardiomyopathies in experimental animals: mechanical, biochemical, and structural features. *Ann NY Acad Sci* 1979;317:59–88.
4. Bajusz E. Hereditary cardiomyopathy: a new disease model. *Am Heart J* 1969;77:686–696.
5. Homburger F, Baker JR, Nixon CW. Primary generalized polymyopathy and cardiac necrosis in an inbred line of Syrian hamsters. *Med Exp* 1962; 6:339–345.
6. Pieri P, Fishman AJ, Ahmad M, Moore RH, Callahan RJ, Strauss HW. Cardiac blood-pool scintigraphy in rats and hamsters: comparison of five radiopharmaceuticals and three pinhole collimator apertures. *J Nucl Med* 1991;32:851–855.
7. Kobayashi A, Yamashita T, Kaneko M, Nishiyama T, Hayashi H, Yamazaki N. Effect of verapamil cardiomyopathy in the Bio 14.6 Syrian hamster. *J Am Coll Cardiol* 1987;10:1128–1134.
8. Factor SM, Cho S, Scheuer J, Sonneblick EH, Malhotra A. Prevention of hereditary cardiomyopathy in the Syrian hamster with chronic verapamil therapy. *J Am Coll Cardiol* 1988;12:1599–1564.
9. Livni E, Elmaleh DR, Levy S, Brownell GL, Strauss HW. Beta-methyl [1-^{11}C] heptadecanoic acid: a new myocardial metabolic tracer for positron emission tomography. *J Nucl Med* 1982;23:169–175.
10. Elmaleh DR, Livni E, Levy S, Varnum D, Strauss HW. Comparison of ^{11}C and ^{14}C-labelled fatty acid and their beta-methyl analogs. *Int J Nucl Med* 1983;10:181–187.
11. Yonekura Y, Brill AB, Som P, et al. Regional myocardial substrata uptake in hypertensive rats: a quantitative autoradiographic measurement. *Science* 1985;227:2492–2496.
12. Yamamoto K, Som P, Brill AB, et al. Dual tracer autoradiographic study of beta-methyl- (1-C-14) heptadecanoic acid and 15-p-(iodophenyl-beta-methylpentadecanoic acid in normotensive and hypertensive rats. *J Nucl Med* 1986;27:1178–1183.
13. Bajusz E, Homburger F, Baker JR, Opie LH. The heart muscle in muscular dystrophy with special reference to involvement of the cardiovascular sys-

tem in the hereditary myopathy of the hamster. *Ann NY Acad Sci* 1966;138: 213–231.
14. Homburger F. Myopathy of hamster dystrophy: history and morphologic aspects. *Ann NY Acad of Sci* 1979;317:2–17.
15. Gertz EW. Pathology of the Syrian hamster progress in experimental tumor research. *Prog Exp Tumor Res* 1972;16:242–260.
16. Lossnitzer K, Janke J, Hein B, Stauch M, Fleckenstein A. Disturbed myocardial calcium metabolism: a possible pathogenetic factor in the hereditary cardiomyopathy of the Syrian hamster. *Recent Adv Stud Card Struc Metab* 1975;6:207–217.
17. Wagner JA, Reynolds IJ, Weisman ML, Dudeck P, Weisfeldt ML, Snyder SH. Calcium antagonist receptors in cardiomyopathic hamster: selective increase in heart, muscle, brain. *Science* 1986;232:515–518.
18. Wagner JA, Weisman HF, Snowman AM, Reynold IJ, Weisfeldt ML, Snyder SH. Alterations in calcium antagonist receptors and sodium calcium exchange in cardiomyopathic hamster tissue. *Circ Res* 1989;65:205–215.
19. Finkel MS, Marks ES, Patterson R, Speir EH, Steadman K, Keiser HR. Increased cardiac calcium channels in hamster cardiomyopathy. *Am J Cardiol* 1986;57:11205–1206.
20. Kuo TH, Tsang W, Weiner J. Defective Ca^{2+}-pumping ATPase of heart sarcolema from cardiomyopathic hamster. *Biochim Biophys Acta* 1987;900: 10–16.
21. Coleman RE, Klein MS, Ahmad SA, Weiss ES, Buchholz WH, Sobel BE. Mechanism contributing myocardial accumulation of technetium-99m stannous pyrophosphate after coronary arterial occlusion. *Am J Cardiol* 1977; 39:55–59.
22. Factor SM, Minse T, Cho S, Dominitz B, Sonnenblick EH. Microvascular spasm in the cardiomyopathic Syrian hamster: a preventable cause of focal myocardial necrosis. *Circulation* 1982;66:342–354.
23. Capasso JM, Sonnenblick EH, Anversa P. Chronic calcium channel blocker prevent the progression of myocardial contractile and electrical dysfunction in the cardiomyopathic Syrian hamster. *Circ Res* 1990;67:1381–1393.
24. Factor SM, Cho S, Scheuer J, Sonneblick EH, Malhotra A. Prevention of hereditary cardiomyopathy in the Syrian Hamster with chronic verapamil therapy. *J Am Coll Cardiol* 1988;12:1599–1564.
25. Wisneski JA, Gertz EW, Neese RA, Mayer M. Myocardial metabolism of free fatty acids. *J Clin Invest* 1987;79:359–366.
26. Fox KAA, Abendschein DR, Ambos HD, Sobel BE, Bergmann SR. Efflux of metabolized and non-metabolized fatty acid from canine myocardium. *Circ Res* 1985;57:232–243.
27. Karlson P. *Introduction to Noderb biochemistry*. London: Academic Press; 1975:242–244.
28. Aswitto RJ, Ross-Ascuitto NJ, Chen V, Downig SE. Ventricular function and fatty acid metabolism in neonatal piglet heart. *Am J Physiol* 1989;256: H9–H15.
29. Wood JM, Sordahl LA, Lewis RM, Schwarz A. Effect of chronic myocardial ischemia on activity of the carnitine palmitoyl-Co: a transferase of isolated canine heart mitochondria. *Circ Res* 1973;32:340–347.
30. Goldstein RA, Klein MS, Wlein MJ. Experimental assessment of myocardial metabolism with C-11 palmitate in vivo. *J Nucl Med* 1980;21:342–348.
31. Fink GD, Montgomery JA, David F, et al. Metabolism of β-Methyl-heptadecanoic acid in the perfused rat heart and liver. *J Nucl Med* 1990;31:1823–1830.
32. Saito T, Yasuda H, Gold HK, et al. Differentiation of regional perfusion And fatty acid uptake in zones of myocardial injury. *Nucl Med Commun* 1991;12:663–675.
33. Fridrich L, Gassner A, Sommer G, et al. Dynamic ^{123}I-HDA myocardial scintigraphy after aortocoronary bypass grafting. *Eur J Nucl Med* 1986;12: S24–S26.
34. Miller DD, Gill JB, Livni E, et al. Fatty acid analogue accumulation: a marker of myocyte viability in ischemic reperfused myocardium. *Circulation Res* 1988;63:681–692.
35. Kubota K, Som P, Oster ZH, et al. Detection of cardiomyopathy in an animal model using quantitative autoradiography. *J Nucl Med* 1988;29: 1697–1703.